Materials Today: Proceedings 46 (2021) 1290–1297

Contents lists available at ScienceDirect

Materials Today: Proceedings

journal homepage: www.elsevier.com/locate/matpr

Finite element analysis of low-velocity impact behavior of green composites

Gorrepotu Surya Rao, Kishore Debnath *, Rabindra Narayan Mahapatra

Department of Mechanical Engineering, National Institute of Technology, Meghalaya, Shillong 793003, India

ARTICLE INFO

Article history:
Available online 27 February 2021

Keywords:
Green composites
Low-velocity impact
Abaqus
Hashin damage criteria

ABSTRACT

This study presents the low-velocity impact behavior of natural fiber-reinforced green composites. The green composite plate was composed of bamboo fiber and polylactic acid (PLA). The green composite plate of 4 mm in thickness was modeled considering unidirectional bamboo fiber. A hemispherical steel indenter of 16 mm in diameter was used to study the impact behavior of green composites using ABAQUS 6.14. The analysis was performed at impact velocities of 2, 2.54, 3.08, and 3.556 m/s by varying the fiber weight percentage to 10, 20, and 30% in the bamboo/PLA green composites. The simulated results were compared with the findings reported in previous studies.

Selection and peer-review under responsibility of the scientific committee of the 28th International Conference on Processing and Fabrication of Advanced Materials.

1. Introduction

The strength and stiffness coupled with lightweight characteristics are the striking features of composites for their widespread applications in the manufacturing sector. Non-toxic nature, durability, chemical and corrosion resistance, compact tolerance, design flexibility, low-cost, and eco-friendly nature are the other attractive characteristics of composites that motivated researchers to use this material in diverse applications. Due to the increasing environmental concern, the research motivation and focus shifted towards the development of green composites. Understanding the damage behavior of this type of composites under different conditions is an area of paramount importance. The damage caused by the impact is categorized into intra-laminar and inter-laminar damage. The debonding between matrix and fiber, cracking of matrix, and fiber breakage comes under intra-laminar damage. Hashin criteria are considered for estimating the intra-laminar damages of composites. Material fracture into layers or delamination of composites is termed as inter-laminar damage. The material properties, structural behavior, and impact parameters like indenter properties significantly influence the damage mechanisms. These types of damages are observed in composite structures depending on the different loading and boundary conditions. The impact damages are not contemplated as a major issue in metals due to their ductile nature. Metal undergo large deformation at constant yield stress before work hardening. Usually, the damage in elastic and plastic regions helps to absorb more energy in metals as compared to composites. The damage mainly restricted to the elastic region causes less amount of energy absorption due to the brittle nature of composites. The susceptibility of impact damage to the composites opens up a new window to examine advanced composites. The estimation of impact damage through simulation helps to find the initial defects and other drawbacks. The damage to the structural properties of composites can be estimated by analyzing the composites. The finite element analysis of composites by ABAQUS is one of the best ways to analyze the models. In the finite element analysis, the model is subdivided into a large number of finite elements. The behavior of individual elements can be estimated for known properties of the composites. The mathematical equations help to add the individual behavior of all finite elements to predict the overall performance of the composites. Ease of modeling, high degree of accuracy, visualization, time-dependent analysis, and adaptability are the main advantages of finite element analysis. Xu and Chen [1] studied the low-velocity impact behavior of carbon/epoxy laminates. The matrix failure and delaminated areas were predicted and compared with the experimental results. Aldajah et al. [2] investigated the low-velocity impact behavior of laminated Kevlar/nanoclay plates. The delamination and failure of the composites were predicted by the von Mises stress failure criterion. Chaht et al. [3] simulated carbon/epoxy composites by using ABAQUS software. The effect of stacking sequence and thick-

* Corresponding author.
E-mail address: debnath.iitr@gmail.com (K. Debnath).

https://doi.org/10.1016/j.matpr.2021.02.130
2214-7853/
Selection and peer-review under responsibility of the scientific committee of the 28th International Conference on Processing and Fabrication of Advanced Materials.

ness of the plate on the damage of composites was verified by using the Hashin damage criterion. Sanga et al. [4] investigated the low-velocity impact of laminated carbon/epoxy composites for aeronautical structures. The damage initiation and propagation were estimated based on Hashin and Benzeggagh-Kenane criteria. The accuracy of the simulated models was compared with experimental results. Bozkurt et al. [5] performed a drop weight test on carbon/epoxy laminated composites. The crack in the matrix of the lower ply was observed at low-velocity impact. The author concluded that simulation accurately predict the delamination region expanding in the same direction of fiber in the lower layer. Belingardi and Vadori [6] investigated low-velocity impact behavior of glass/epoxy composites. The mechanical characteristics, impact force history, and energy parameters were used to study the impact behavior of the composites. Sun et al. [7] examined the glass/epoxy-SMA-based composites under low-velocity impact test. The author compared the experimental and simulated results of composites by considering different impact energies. At low impact energy, the damage to the composites was observed by the matrix cracks. The fiber breaking was observed due to the penetration of indenter at high impact energy. Guida et al. [8] performed low-velocity impact test on hybrid and CFRP composites for aeronautical applications. The energy absorption by both hybrid and CFRP composites was the same when subjected to low-velocity impacts. The delamination area of the CFRP composites specimens was much more extended as compared to the hybrid composites. Mathivanan and Jerald [9] examined the impact resistance of GFRP composites. GFRP composites exhibited better impact toughness as compared to graphite-based GFRP composites at low-velocity impact. The energy absorption rate was the same in both composites during the impact testing. Bandaru et al. [10] performed experimental and simulated investigation on low-velocity impact response of hybrid composites. The basalt fiber front faced hybrid composites was performed better in terms of energy absorption and peak force as compared to the Kevlar fiber front faced hybrid composites. Li et al. [11] investigated carbon/epoxy composites laminates under low-velocity impact testing. The inter-laminar damage of matrix and fiber was evaluated using Puck criterion. Ribeiro et al. [12] examined the simulated results by implementing different failure modes like fiber failure and inter-fiber failures. The fiber failure issues and parameters causing degradation to the properties of composites were observed. Mohmmed et al. [13] investigated the impact damage response of foam sandwiched composites with different ply angles. A crucible foam model was created to simulate the composites under the low-velocity impact. Hashin criteria were used to estimate the damage response on the faces of the composites. The damage size, damage shape, and failure on the faces of the composites were assessed and compared with experimental results by collecting the loading history and absorbed energy rate. Shi and Soutis [14] reported that under the low-velocity impact, intra- and inter-laminar cracks were developed on the carbon/epoxy composites. Abdel-Nasser et al. [15] investigated the behavior of glass/epoxy composites under high and low-velocity impact testing. The verification of real impact cases helped to explain the necessity of boundary condition selection for estimating the failure modes. The author concluded that the utilization of high strength materials resulted in reduction in the weight of the composite plate. Du et al. [16] examined the intra-laminar stresses and inter-laminar damages of carbon/epoxy composites by performing low-velocity impact test. The matrix damage and delamination area of the composite plate were predicted and compared with experimental values. Song et al. [17] investigated the performance of carbon incorporated aluminum laminate modeled by ABAQUS under the low-velocity impact range. The impact response of modeled plate was estimated by energy-time history values. The author utilized the impact of load-time history to compare the experimental results with simulated models. Rathnasabapathy et al. [18] studied aluminum-glass fiber composites performance by varying impact energies. The plastic deformation was observed in the aluminum layers due to its ductile nature. The fiber breakage, cracks, and delamination of the composites were also observed. Pashmforoush [19] examined the effect of carbon nanotubes (CNT) on the carbon fiber-reinforced composites at low-velocity impact range. The addition of CNT to the composites resulted in less damage to the composite plate. The author also concluded that more addition of CNT causes debonding between the ply layers of the composites which resulted in decrease in the impact resistance. Alemi-Ardakani et al. [20] investigated the impact damage of glass fiber-reinforced composite plate using ABAQUS. The finite element analysis of modified material properties and quasistatic model responses were compared with experimental results. Maji et al. [21] reported that quadratic stress-based criteria helped to estimate the intra-laminar damage of the carbon/epoxy composites at low-velocity impact testing. The delamination and absorbed energy rate was predicted and compared with the experimental values. Mars et al. [22] examined the impact response of modeled glass/polyamide composites by ABAQUS. It was found that the effect of increase in the fiber volume fraction and impact velocity is directly proportional to the impact force response.

It is quite clear from the above literature review that most of the researchers focused on the low-velocity impact response of synthetic composites. The impact behavior of green composites has not been investigated though these materials have wide application spectrum. Thus, in this study, green composites composed of bamboo fiber and PLA was modeled using ABAQUS 6.14 [23]. The effect of varying impact velocities and fiber weight percentage on the composites was simulated. Hashin damage criteria were used to estimate the intra-laminar damages on the composite plate. The simulated results of the green composite plate were also compared with the experimental results of previous studies.

2. Modeling and simulation

2.1. Mechanical properties of materials

The mechanical properties of individual constituent of composites define the performance of the composites. The mechanical properties of the composites also depend on the interfacial bonding between the matrix and fiber. In this study, bamboo fiber and PLA were considered as reinforcement and binding material for modeling a green composite plate. The bamboo fiber was reinforced with PLA in different weight percentage (10 to 30%). The eco-friendly and biodegradability characteristics are the main reasons to select PLA and bamboo fiber. The properties of PLA and bamboo fiber were collected from the ANSYS database. The mechanical properties of PLA and bamboo fiber are shown in Table 1 and Table 2, respectively.

Table 1
Physical and mechanical properties of PLA.

Properties	Values	Units
Density	1250	kg/m^3
Coefficient of thermal expansion	0.000135	$°C^{-1}$
Young's modulus	3.45E + 09	Pa
Poisson's ratio	0.39	–
Bulk modulus	5.2273E + 09	Pa
Shear modulus	1.241E + 09	Pa
Tensile yield strength	5.41E + 07	Pa
Tensile ultimate strength	5.92E + 07	Pa
Thermal conductivity	0.144	J/ms°C
Specific heat	1190	J/kg°C

Table 2
Physical and mechanical properties of bamboo fiber.

Properties	Values	Units
Density	693	kg/m^3
Coefficient of thermal expansion	3.26E-6	°C^{-1}
Young's modulus	1.73E + 10	Pa
Poisson's ratio	0.384	–
Bulk modulus	2.4856E + 10	Pa
Shear modulus	6.25E + 09	Pa
Tensile yield strength	3.97E + 07	Pa
Tensile ultimate strength	2.26E + 08	Pa
Thermal conductivity	0.17	J/ms°C
Specific heat	1680	J/kg°C

2.2. Estimation of composites properties

The rule of mixture is a method used to estimate the overall properties of composites by considering the individual properties of matrix and fiber. In rule of mixture, the prediction of properties is based on the weight contributions of the matrix and fiber. The rule of the mixture is fairly a simple and accurate method to estimate the properties of the composites. The assumptions considered to estimate the properties of composites are (i) adequate interfacial bonding between the fiber and matrix, (ii) strain rate in the matrix and fiber is the same under the application of longitudinal load, (iii) application of load is always perpendicular to the fiber while estimating transverse parameters, (iv) fiber alignment is uniform and perfectly parallel to the plane, (v) no voids present in the composites, and (vi) shape and size of the fiber are unique and systematically spaced. The mechanical properties of unidirectional fiber composites were predicted by varying the fiber weight percentage as 10, 20, and 30%. The young's modulus in different directions, poison's ratio, shear modulus, density, and thermal conductivity of the bamboo/PLA composites were predicted using the rule of mixture. Table 3 shows the different properties of bamboo/PLA composites.

2.3. Hashin damage criteria

The simulation of composites is quite difficult. The microstructure of the composite plate keeps on changing due to continuously increasing the applied stress. The damage to the composites mainly occurs in the form of matrix cracking, fiber breaking, and delamination. Hashin criteria are preferred to estimate the damage modes on the composites by more than one stress components. This criterion is specifically used to predict the damage on unidirectional fiber-reinforced composites. The different modes of failures in Hashin damage criteria are related to the damage in fiber and matrix. The different modes of failure in Hashin damage criteria are (a) tensile fiber failure ($\sigma_{11} \geq 0$), (b) compressive fiber failure ($\sigma_{11} < 0$), (c) tensile matrix failure ($\sigma_{22} + \sigma_{33} > 0$), (d) compressive matrix failure ($\sigma_{22} + \sigma_{33} < 0$), (e) inter-laminar tensile failure ($\sigma_{33} > 0$), and (f) inter-laminar compressive failure ($\sigma_{33} < 0$). In ABAQUS, the input parameters considered to execute Hashin damage are longitudinal tensile and compressive strengths (X_t, X_c), transverse tensile and compressive strengths (Y_t, Y_c), and longitudinal and transverse shear strengths (X_s, Y_s). All the input parameters were calculated using the physical and mechanical properties of bamboo/PLA composites. Table 4 shows the values of different strength parameters of composites based on the fiber weight percentage.

3. Modeling of composite plate

A three-dimensional deformable composite plate of 150 × 150 × 4 mm was modeled in ABAQUS to perform the simulation. The properties of bamboo/PLA composites were assigned to the plate. The failure behavior of composites was determined under impact loading. In the material section, all strength values were entered to estimate the damage of the composites in different modes. A hemispherical steel indenter of 16 mm in diameter was modeled to perform the low-velocity impact test on the composite plate. The properties of steel were assigned to the indenter. The composite plate and the indenter were assembled with a surface contact with respect to a reference point as shown in Fig. 1. The mass of the indenter (1.265 Kg) was allocated by creating a reference point on the surface of the hemispherical indenter. Table 5 shows the mechanical properties of the indenter. The interaction between the top surface of the modeled plate and the bottom surface of the indenter was created by defining the interaction properties. The interaction is normal behavior with a frictional penalty of 0.3 between the indenter and composite plate. In the boundary conditions, the outer edges of the composites were fixed by entering the displacement zero in all directions. The indenter moment was constrained in X and Y directions by fixing the corresponding displacement and rotation as zero. The indenter is free to move in the Z direction to create an impact on the composite plate.

The impact test was performed on the plate by varying the indenter velocities as 2, 2.54, 3.08, and 3.556 m/s. The kinetic energies were estimated at different impact velocities. The corresponding kinetic energy values are 2.53, 4.0, 6.0, and 8.0 J. The uniform mesh was generated in the composite plate with a mesh size of 4 mm. In the step function, the output responses were selected before performing the simulation. The output responses like reaction forces, translational displacements, stress, and strain components were considered. For analyzing the failure of the simulated plate, Hashin output responses like Hashin's fiber tensile damage initiation criteria (HSNFTCRT), Hashin's fiber compressive damage initiation criteria (HSNFCCRT), Hashin's matrix tensile damage initiation criteria (HSNMTCRT), and Hashin's matrix compressive damage initiation criteria (HSNMCCRT) were selected.

4. Results and discussion

The impact behavior of bamboo/PLA composite plate with 10, 20, and 30 wt% fiber content was simulated. The effect of impact velocity on the composite plate was also studied. The impact response of the composite plate was evaluated in terms of maximum impact force and displacement. The effect of varying fiber content and impact velocity on the damage to the composite plate was also evaluated using Hashin damage criteria. Fig. 2 shows the maximum force versus initial velocity of the indenter. The increase in the force is proportional to the velocity for all the composite plate modeled with fiber content of 10, 20, and 30 wt%. The response of the force and time history of the composite plate at

Table 3
Physical and mechanical properties of bamboo/PLA composites.

Fiber wt.%	E_1 (GPa)	E_2 (GPa)	ν	$G_{12} = G_{13}$ (GPa)	G_{23} (GPa)	Density (kg/m^3)	Thermal conductivity (J/m.s.c)
10	4.835	4.1366	0.38	1.4675	1.3788	1194.3	0.14623
20	6.746	5.0802	0.3885	1.8297	1.7398	1138.6	0.1494
30	7.955	6.8014	0.3874	2.4494	2.4323	1082.9	0.15409

Table 4
Strength values of composites for Hashin criteria.

Fiber wt.%	X_t (MPa)	Y_t (MPa)	X_c (MPa)	Y_c (MPa)	X_s (MPa)	Y_s (MPa)
10	219.3	18.6721	99.1759	77.09538	27.15	27.1524
20	470.874	16.151	136.7162	75.0149	26.4	26.4999
30	818.1555	13.1966	163.4104	76.8059	27.0	27.0336

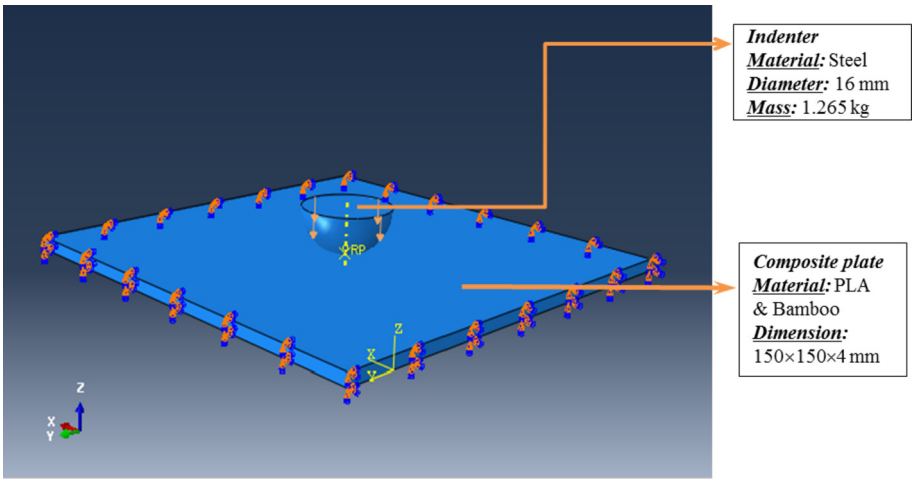

Fig. 1. Geometry and boundary conditions of composite plate and indenter.

Table 5
Mechanical properties of the indenter.

Material	Mass (kg)	Density (kg/m^3)	Poisson's ratio	Young's modulus (GPa)
Steel	1.265	7800	0.3	200

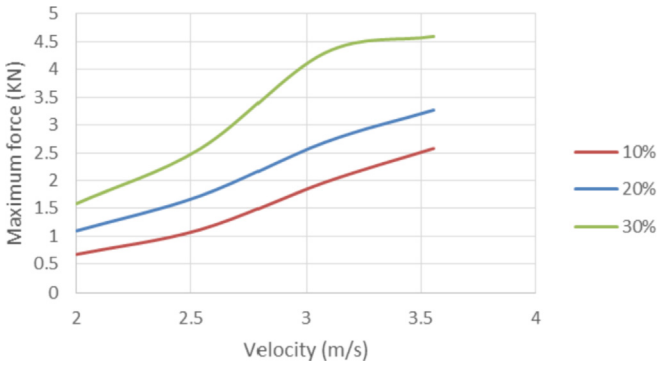

Fig. 2. Maximum force response with respect to initial indenter velocity.

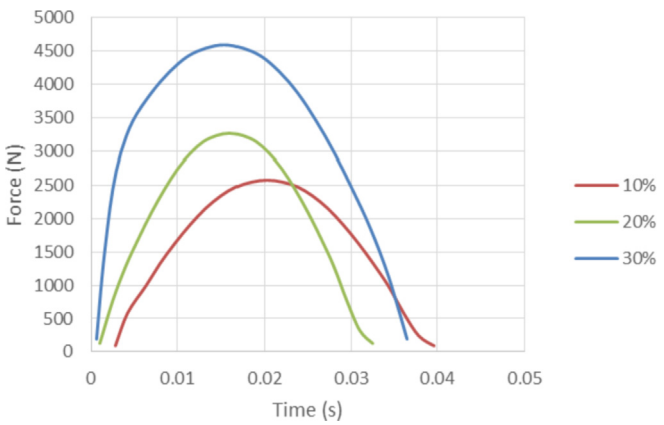

Fig. 3. Force vs. time curve for an impact velocity of 3.556 m/s.

the maximum velocity of 3.556 m/s is shown in Fig. 3. The force was more in composite plate consists of fiber weight percentage of 30% as compared to 10 and 20%. From the graph, it is clear that the force initially increases to a certain level and attains the maximum value. Then the force decreases gradually with respect to time. The increase in force indicates that the composite plate is bearing the load offers by the indenter. The sudden fall in force after attaining the maximum value is an indication of damage to the composite plate. The maximum force obtained at different velocity of indenter for different composite plate is shown in Table 6. The force–time response describes the damage initiation, damage propagation, and stiffness reduction of the composite plate [10]. The sudden drop in force after the impact results in damage initiation through matrix cracking.

To verify the accuracy of the developed model, the present simulated results were compared with the published work where a thin composites disc was simulated with different frictional coefficient values [12]. The tangential interaction force was increased with frictional coefficient (0.1 to 0.3) which resulted in an increase in the maximum force. The higher tangential reaction developed due to increase in the frictional coefficient between the indenter and composite plate. The maximum force of 3691 N was obtained at 3.9 m/s for undamaged composites. CFRP composites impacted by 2.35 and 9.40 J energy levels deform 0.47 and 1.49 mm, respectively [17]. The maximum force increased with respect to the

Table 6
The force response with respect to different fiber content and velocity.

Fiber wt.%	Velocity of indenter (m/s)			
	2	2.54	3.08	3.556
	Maximum force (kN)			
10	0.6728	1.118	1.968	2.578
20	1.098	1.726	2.688	3.270
30	1.588	2.527	4.299	4.597

impact energy. The maximum force reached to 2438 N at 2.35 J and 4512 N at 9.40 J. No critical damage was observed at 2.35 J. At the maximum energy of 9.40 J, shear damage and fiber cracks were observed in the plate. The carbon/epoxy composites with initial impact energy of 14.7 J attained the maximum force of 3917 N [14]. Due to the elastic behavior, mild oscillations were observed between the indenter and composites. After reaching the maximum force, extreme oscillations were noticed and confirmed the damage initiation in the composite plate. Fig. 4 shows that the displacement of the composites modeled with 30 wt% fiber was more than the other composite plates. The maximum displacement for 30 wt% bamboo/PLA composites was found at the impact velocity of 3.556 m/s. The force was increased in the elastic region (Fig. 5). After reaching the maximum value, the force decreased with respect to displacement. It was clear that the load was successfully born by the composite plate under low-velocity impact. The maximum range of displacement was observed between 2 and 9 mm for glass/polyamide composites under impact loading [22]. The maximum force variation observed from the force and time history graphs were 2.5 to 3.5 kN at 3.556 m/s. The maximum displacement range was 20 to 25 mm for GRPF composites at an impact velocity of 2.215 m/s [9]. The impact test on GFRP at an indenter velocity of 3.132 m/s exhibited maximum force of 1822.5 N. The matrix cracking was observed due to the generation of maximum force. The displacement was between 7 and 14 mm with the varying CNT percentage in CFRP composites [19]. The carbon/epoxy foam sandwiched composites simulated under low-velocity impact showed the maximum force of 3.25 kN at 15 J [13]. The damage to the composites was observed at the top surface of the foam without further damage to the next layers of composites. But the load–displacement curve of unidirectional composites showed three layers of damage. The simulated carbon/epoxy composites showed maximum force of 3000 N with

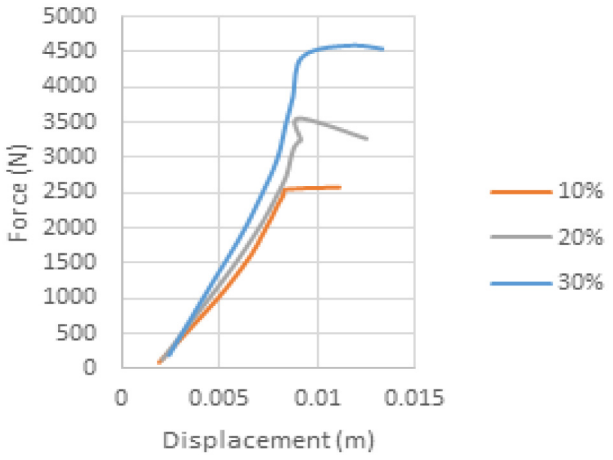

Fig. 5. Force vs. displacement at 3.556 m/s.

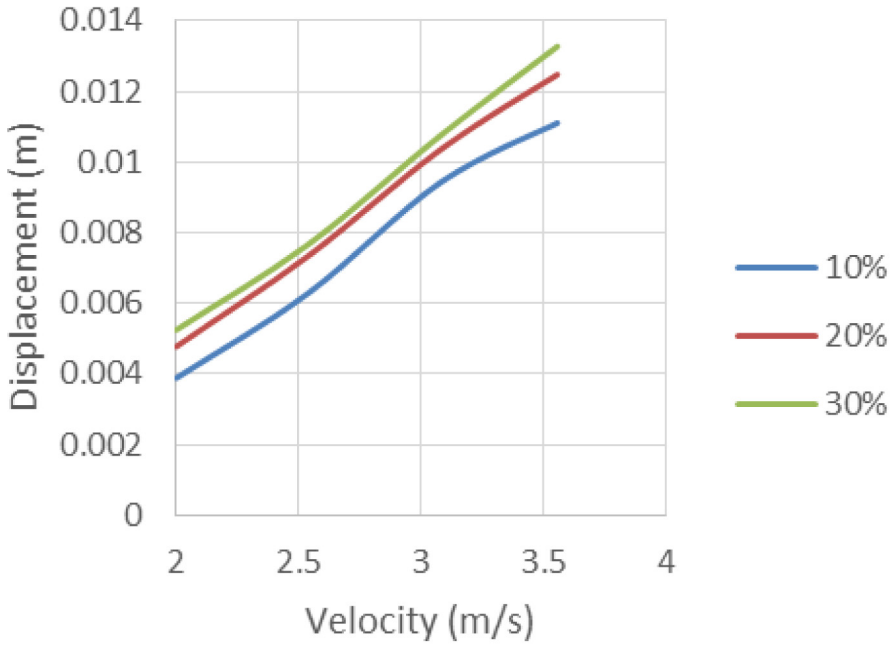

Fig. 4. Displacement vs. velocity.

Table 7
The maximum force reported with respect to velocity in previous studies.

Composite	Maximum Force (N)	Velocity (m/s)	Reference No.
CFRP	3691	3.90	[12]
Carbon/epoxy	3917	4.83	[14]
CFRP	4512	3.86	[17]
Glass/epoxy	6500	3.50	[18]
Glass/polyamide	3500	3.56	[22]

Table 8
The displacement reported with respect to velocity in previous studies.

Composite	Displacement (mm)	Velocity (m/s)	Reference No.
GFRP	20–25	3.90	[9]
CFRP (Varying CNT %)	7–14	3.86	[13]
Glass/polyamide	9	3.56	[22]

an indenter weight of 1.28 kg [16]. At the maximum force, more vibrations were observed which led to matrix cracking. After that, the force was decreased due to formation of small cracks in the matrix and damage to the fiber. The impact analysis on aluminium with glass/epoxy composites showed the maximum force of 6.5 kN [18]. Increasing the impact energy resulted in more damage and plastic deformation of the aluminium layers coupled with matrix cracking and fiber damage. The above discussion shows that the results of the present work corroborate the finding of previous works in Tables 7 and 8.

4.1. Hashin damage criteria of modeled plates

The effect of fiber content and indenter velocity on the composite plate is shown in Figs. 6–9. The figures show the damage modes of composite plate composed of 20 wt% bamboo fiber at different impact velocities. The figures are sequentially arranged from left to right as fiber compressive damage initiation, fiber tensile damage initiation, matrix compressive damage initiation, and matrix tensile damage initiation. Fiber and matrix are the main constituents of composites. The applied load is majorly carried by the fiber. The matrix transfers the load to the fiber and protects the fiber from damage. The strength and stiffness of the composites are estimated by the load-bearing capacity of the fiber and the interfacial bonding strength between the fiber and matrix. A decrease in the bonding strength between matrix and fiber due to the formation of cracks in the matrix led to failure of matrix at low-velocity impact. The fiber failure was more in the contact region between the indenter and composite plate. More bending stress developed in the un-impacted region of the composite plate and thus failure of fiber was the minimum in that region. The failure of the fiber was more due to the developed indentation stress in the contact region between the indenter and composite plate. In this study, the fiber compression was restricted in the contact region between the indenter and composite plate. The damage due to fiber compression was increased with fiber content. The indenter movement was perpendicular to the fiber direction which caused fiber compression in the contact region of indenter and composite plate. In all the cases, minor fiber tensile damage was observed. The increase in the force caused more bending stress on the composite plate. The application of load was perpendicular to the fiber direction caused tension in the fibers. The fibers of the composite plate crushed due to the bending of the plate under impact loading. Due to this effect, fiber will compress under the indenter. Outside the impact region, the fibers of the composite plate were under tension. The matrix compression damage was less in the composites composed of 10 wt% bamboo fiber. Matrix compression damage was not observed with an increase in the velocity up to 2.54 m/s. Further increase in the velocity to 3.556 m/s resulted in matrix compression damage to the compos-

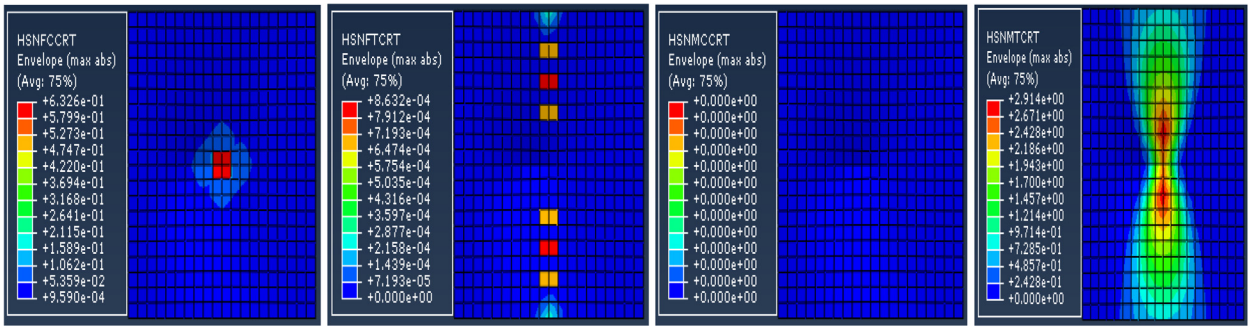

Fig. 6. Damage to the composite plate composed of 20 wt% bamboo fiber at an impact velocity of 2 m/s.

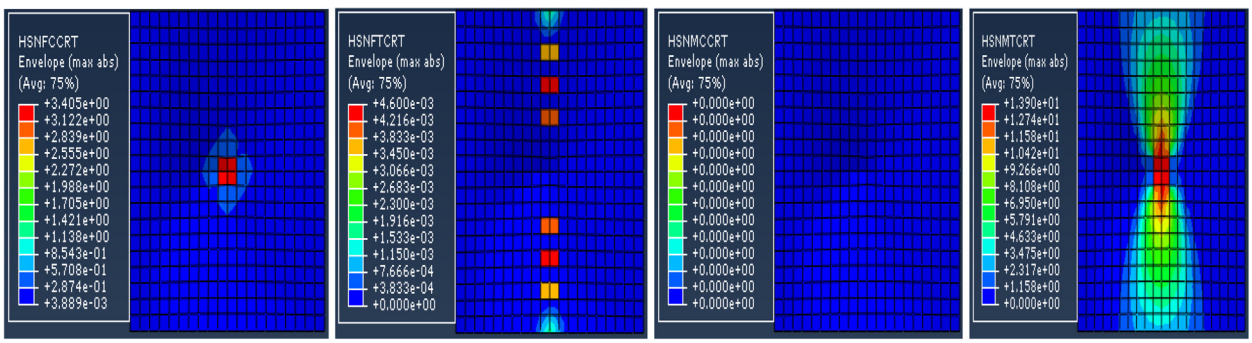

Fig. 7. Damage to the composite plate composed of 20 wt% bamboo fiber at an impact velocity of 2.54 m/s.

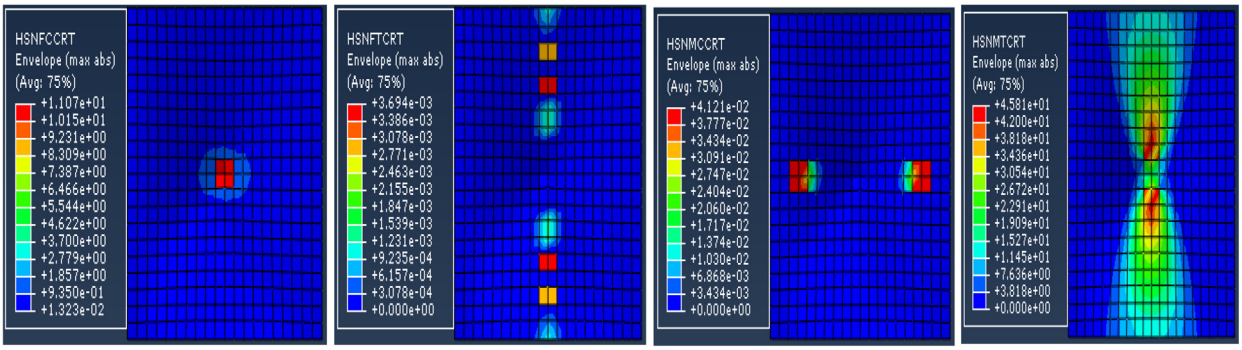

Fig. 8. Damage to the composite plate composed of 20 wt% bamboo fiber at an impact velocity of 3.08 m/s.

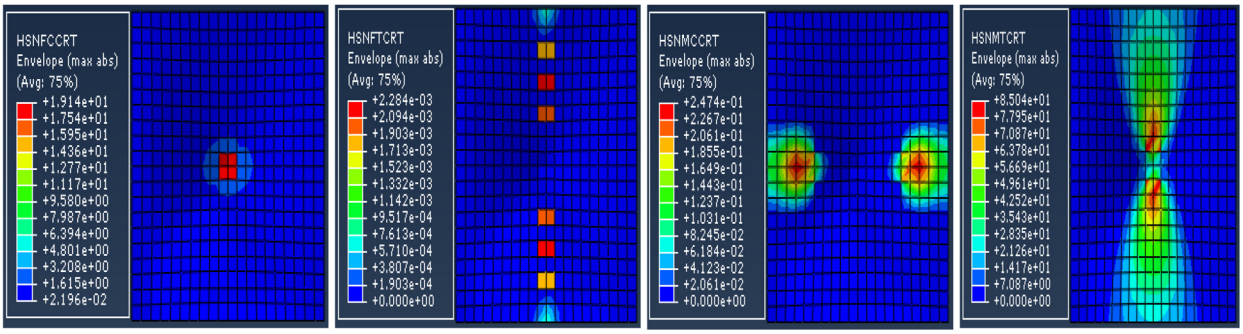

Fig. 9. Damage to the composite plate composed of 20 wt% bamboo fiber at an impact velocity of 3.556 m/s.

ite plate. No damage to the composite plate was observed due to matrix compression at 2.54 m/s. The damage to the CNT-based CFRP composite plate occurred at the center of the plate. No significant damage was observed due to matrix compression [19]. Noticeable fiber compression damage was observed with an increase in the CNT percentage. All the plies were damaged under matrix tension. More matrix tensile damage to the composite plate was observed with an increase in the velocity of the indenter. The developed compressive stress in the contact region between the indenter and composite plate caused matrix tension. The tension in the un-impacted region increased gradually which resulted in more tension in the matrix with an increase in velocity of the indenter. The bending deformation was observed in carbon/epoxy composite plate away from the impacted region [11]. Matrix cracks were observed in all the plies due to the developed stress. In all cases, less damage was observed under fiber compression and tension due to the impact of the indenter. Most of the damage occurred to the composite plate by the matrix tension and negligible damage was observed due to matrix compression under low-velocity impact.

5. Conclusion

The present study investigates the low-velocity impact behaviour of bamboo/PLA green composites. The influence of the fiber weight percentage and velocity of the indenter on the composite plate was examined. Low-velocity impact test was performed at different velocities of the indenter. From the study, it was found that the fiber loading and velocity of the indenter were directly proportional to the maximum force. The maximum force increased as the fiber weight percentage increase from 10 to 30%. The response of the maximum force with respect to velocity, time, and displacement was found to be in close agreement with the previous studies. The intra-laminar damages of the composite plate were also verified. Damages to the composite plate occurred due to the effect of fiber tension and compression. Negligible damage to the composite plate was observed under matrix compression. The previous reports also showed that the main damage to the composites occurred because of the matrix tension.

Declaration of Competing Interest

The authors declare that they have no known competing financial interests or personal relationships that could have appeared to influence the work reported in this paper.

Acknowledgements

All persons who have made substantial contributions to the work reported in the manuscript (e.g., technical help, writing and editing assistance, general support), but who do not meet the criteria for authorship, are named in the Acknowledgements and have given us their written permission to be named. If we have not included an Acknowledgements, then that indicates that we have not received substantial contributions from non-authors.

References

[1] S. Xu, P.H. Chen, Procedia Eng. 67 (2013) 489–496.
[2] S. Aldajah, Y. Haik, K. Moustafa, A. Alomar, Int. J. Eng. Technol. 6 (2014) 258–261.
[3] F.L. Chaht, M. Mokhtari, H. Benzaama, Frattura ed Integrità Strutturale 13 (2019) 331–341.
[4] R.P.L. Sanga, C. Garnier, O. Pantalé, Appl. Compos. Mater. 23 (2016) 1195–1208.
[5] M.O. Bozkurt, L. Parnas, D. Coker, Procedia Struct. Integr. 21 (2019) 206–214.
[6] G. Belingardi, R. Vadori, Int. J. Impact Eng. 27 (2002) 213–229.
[7] M. Sun, M. Chang, Z. Wang, H. Li, X. Sun, Appl. Sci. 8 (2018) 2405.
[8] M. Guida, A. Sellitto, F. Marulo, A. Riccio, Mater. 12 (2019) 153.
[9] N.R. Mathivanan, J. Jerald, J. Miner. Mater. Characteriz. Eng. 11 (2012) 321.
[10] A.K. Bandaru, S. Patel, S. Ahmad, N. Bhatnagar, J. Compos. Mater. 52 (2018) 877–889.

[11] N. Li, P.H. Chen, Q. Ye, Aeronaut. J. 121 (2017) 515–532.
[12] M.L. Ribeiro, R.A. Agélico, R. Medeiros, V. Tita, Int. J. Compos. Mater. 3 (2013) 59–70.
[13] R. Mohmmed, F. Zhang, B. Sun, B. Gu, Mater. Des. 47 (2013) 189–199.
[14] Y. Shi, C. Soutis, Aeronaut. J. 116 (2012) 1331–1347.
[15] Y. Abdel-Nasser, A.M. Elhewy, I. Al-Mallah, Ships Offshore Struct. 12 (2017) 219–226.
[16] J. Du, Y. Tie, C. Li, X. Zhou, Mater. Phys. Mech. 27 (2016) 195–204.
[17] S.H. Song, Y.S. Byun, T.W. Ku, W.J. Song, J. Kim, B.S. Kang, J. Mater. Sci. Technol. 26 (2010) 327–332.
[18] M. Rathnasabapathy, A.P. Mouritz, A.C. Orifici, In Proceedings of 18th International Conference on Composite Materials, 2011.
[19] F. Pashmforoush, J. Appl. Comput. Mech. 6 (2020) 383–393.
[20] M. Alemi-Ardakani, A.S. Milani, S. Yannacopoulos, Sci. World J. (2014).
[21] A. Maji, S. Nimje, K. Akella, Int. J. Mech. Product. Eng. 6 (2018) 69–73.
[22] J. Mars, E. Chebbi, M. Wali, F. Dammak, Compos. B Eng. 146 (2018) 116–123.
[23] http://130.149.89.49:2080/v6.14/books/usb/default.htm (Last accessed on 12th January, 2021).